The 23rd IEEE International Symposium on Robot and
Human Interactive Communication
August 25-29, 2014. Edinburgh, Scotland, UK,

Learning Force and Position Constraints in Human-robot Cooperative Transportation

Leonel Rozo[1], Sylvain Calinon[1,2] and Darwin G. Caldwell[1]

Abstract— **Physical interaction between humans and robots arises a large set of challenging problems involving hardware, safety, control and cognitive aspects, among others. In this context, the cooperative (two or more people/robots) transportation of bulky loads in manufacturing plants is a practical example where these challenges are evident. In this paper, we address the problem of teaching a robot collaborative behaviors from human demonstrations. Specifically, we present an approach that combines: probabilistic learning and dynamical systems, to encode the robot's motion along the task. Our method allows us to learn not only a desired path to take the object through, but also, the force the robot needs to apply to the load during the interaction. Moreover, the robot is able to learn and reproduce the task with varying initial and final locations of the object. The proposed approach can be used in scenarios where not only the path to be followed by the transported object matters, but also the force applied to it. Tests were successfully carried out in a scenario where a 7 DOFs backdrivable manipulator learns to cooperate, with a human, to transport an object while satisfying the position and force constraints of the task.**

I. INTRODUCTION

Robots are often envisaged as human-like machines that can interact with people in a natural and safe way. Such human-robot interaction (HRI) implies that the robot is able to communicate with the person, understand his/her needs and behave accordingly. This impression is particularly important in situations where a human needs the help of another person to perform a given task successfully. For example, the transportation of bulky objects demands at least two persons to carry the load cooperatively. This task may become difficult when the load has to pass through narrow spaces, and even more laborious if the object is fragile enough so that the transporters must concern about the force they apply to it. In this scenario, one of the humans may be replaced by a robotic agent, where the reasoning and adaptation abilities of the human can be combined with the robot's strength and precision. Such functionality may be achieved by programming the robot from demonstrations of the task. Once the collaborative behavior has been learned, the robot can autonomously perform the task, expanding its own skills.

Programming by demonstration (PbD) [1] has been successfully applied to settings where a robot reproduces a learned skill in a standalone fashion [2], [3]. However, this approach has rarely been used in human-robot collaboration

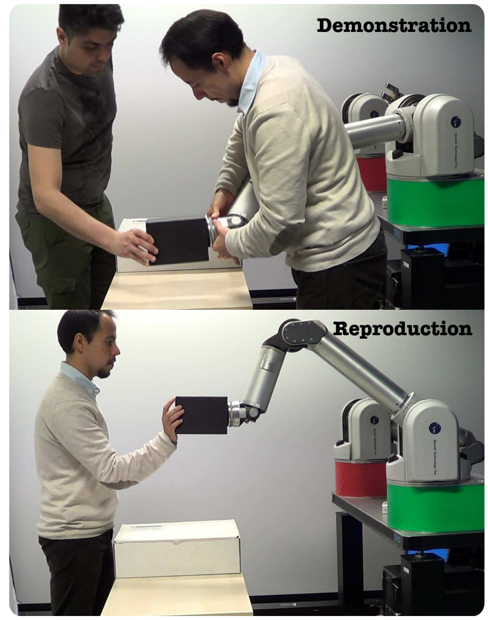

Fig. 1: Experimental setting: demonstration and reproduction phases.

(HRC) scenarios, where control-based solutions have dominated (see Section II). Yet, most control methods require a model of the task, which becomes complex when a human is in the loop. In such instances, PbD emerges as a promising alternative solution allowing the natural transfer of human knowledge about the task to the robot. In this context, a human teacher may, for instance, demonstrate to the robot its role in the task [4], a trajectory to follow [5], or even how compliant it should be [6].

We therefore propose to use PbD to teach a robot to simultaneously handle position and force constraints arising when a human and a robot cooperatively manipulate/transport an object (see Fig. 1). Specifically, our approach defines a set of virtual dynamical systems representing the constraints of the task, and driving the robot motion. Such systems can act on different frames of reference, for instance, on coordinate systems representing the robot's base, the transported object, etc. To deal with this problem, we use a task-parametrized formulation of a Gaussian mixture model that allows us not only to encode the human demonstrations, but also, to extract automatically the importance of the constraints acting at different coordinate systems along the task [7]. Moreover, our approach provides both open-loop and feedback components. This is specially important in HRC, due to the fact that pure open-loop systems cannot react to perturbations, and pure feedback frameworks will impede the speed and fluency of

[1]Department of Advanced Robotics, Istituto Italiano di Tecnologia (IIT), Via Morego 30, 16163 Genova, Italy. name.surname@iit.it
[2]Idiap Research Institute, Rue Marconi 19, PO Box 592, CH-1920 Martigny, Switzerland. sylvain.calinon@idiap.ch
This work was supported by the STIFF-FLOP European project (FP7-ICT-287728) and by the SAPHARI European project (FP7-ICT-287513).

the collaboration. We successfully test our approach in a real-world scenario where a 7 DOFs robotic manipulator learns to perform a cooperative task requiring different force and position constraints to be satisfied.

A brief review on works dealing with similar HRC problems is given in Section II. Details about our approach can be found in Sections III and IV, while results for the cooperative transportation experiment are shown in Section V. Conclusions and future work are presented in Section VI.

II. RELATED WORK

A. Control-based approaches

Human-robot collaboration has been investigated from the early nineties, when purely control-based approaches were dominant. Kosuge *et al.* [8] proposed an impedance control based on the apparent mechanical impedance of an object manipulated by multiple robots and a human. The force applied by the human was transferred to the robot controllers, so that the human could command the motion of the object while the robots behave as followers. The proposed controller was compared against different classic control scheme, where its low damping version performed the best [9].

Al-Jarrah and Zheng introduced a two-levels control schema, where an admittance controller is driven by a higher level force control. The idea here was to trigger a reflex controller when the robot acted as a load for the human by setting a force-based threshold that governs the motion of the manipulator [10]. Duchaine and Gosselin [11] considered that the human intention in cooperative tasks is typically based on the direction and magnitude of the force measured at the robot's end-effector. They proposed to add the rate of change of the sensed force to an impedance controller [12], while varying its damping as function of the changes of magnitude of the force.

Dumora *et al.* decomposed a collaborative task into a sequence of non-holonomic robot motions [13]. Every motion primitive was represented by a predefined virtual mechanism coupled to the robot's impedance controller. Hence, the whole task could be carried out by sequencing the different primitives according to the user's intention [14]. Note that the key feature in all these works has been the need for a model of the task linked to an analysis of the possible robot movements, so that both the parameters and the structure of the controller can be designed accordingly. Unfortunately, most of these frameworks are not flexible, in the sense that if a new task is required or if an additional constraint needs to be considered, the controllers need to be redesigned.

B. Human performance-based approaches

Several works rely on human-human collaboration studies to assist in design of the robot controllers. Ikeura *et al.* proposed to approximate human cooperation using variable impedance control (with zero stiffness). From data collected when two people carried an object, the damping parameter was estimated according to the precision required by the task, either from least squares [12], or by minimizing a cost function that penalized high rates of change [15]. The approach was then improved by introducing stiffness into the controller [16]. Here, the parameters were estimated from force and position data collected when a single human completed the task following minimum jerk robot movements (i.e., the robot acted as the leader while the human was the follower). Note that the minimum jerk model [17] has also been an inspiration for Maeda *et al.* [18]. They proposed to use such a model to estimate the human hand position in a human-robot carrying task. This estimation was used as the reference for the robot impedance controller.

Tsumugiwa *et al.* [19] used an impedance controller, where the damping varied according to the estimate of the human arm stiffness. Their approach assumed that a low velocity cooperative system remains stable if the robot's damping proportionally varies as the human stiffness. Parker *et al.* [20], unlike former works, proposed to iteratively tune the parameters of the robot's admittance controller from the user's preferences with regards to the robotic partner.

Notice that the idea behind all these approaches is mainly to *emulate* the way humans act in a collaborative scenario. This aim has been achieved either by shaping the parameters of a predefined controller using motion/force patterns sensed while a human-human pair carries out the task, or by tuning the controller based on users' feedback. The success of these methods mainly relies on how well the robot controller fits the human collaborative behavior.

C. Learning-based approaches

Evrard *et al.* [4] proposed a probabilistic framework based on Gaussian mixture models (GMM) and Gaussian mixture regression (GMR) to respectively encode and reproduce robot collaborative behaviors. The main idea was to demonstrate, by teleoperation, the leader/follower roles during a cooperative lifting task. GMM encapsulated the robot motion and the sensed forces, whilst GMR generated the reference inputs corresponding to a given sensed force during reproduction. On the other hand, Medina *et al.* [5] endowed their robot with a cognitive system, which provided segmentation, encoding and clustering capabilities for demonstrations of collaborative behavioral primitives. These were represented by a primitive graph and a primitive tree using hidden Markov models (HMM) that were incrementally updated during reproduction [21]. One of the main differences with respect to [4] was that here the robot started behaving as a follower, but its role became more proactive as it acquired more knowledge about the task.

Gribovskaya *et al.* [22] proposed a hybrid structure based on PbD and adaptive control that drives the robot using an adaptive impedance controller. First, a model of the task was learned from demonstrations encoded by a GMM to generate feedforward control signals. Then, the impedance parameters were adapted as function of the kinematic and force errors generated during the execution of the task.

In contrast to the work presented above, where the trajectory to be followed mattered, we proposed in [6] to teach different compliance levels to a robot by kinesthetic teaching.

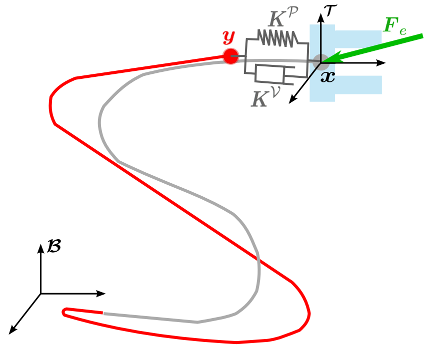

Fig. 2: Illustrative example of the robot motion driven by a virtual spring-damper attractor and constrained to external interaction forces. The gray line represents the demonstrated path of the end-effector. The red line depicts the trajectory of the attractor $\boldsymbol{y}$.

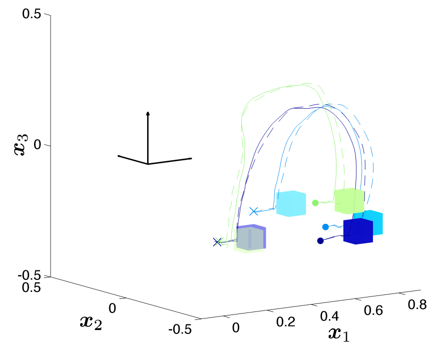

Fig. 3: Three different demonstrations of the collaborative transportation task. The solid and dashed lines respectively depict the end-effector and attractor trajectories. The start and the end of robot motion are represented by colored dots and crosses. The dark and light boxes show the starting and target locations of the transported object.

The core idea was to virtually connect the robot's end-effector to a set of virtual springs driving the robot behavior. A task-parametrized GMM [7] encoding the demonstrations defined the equilibrium points of this system. The model was then augmented by including stiffness matrices estimated from the training data. Yet, no restrictions regarding the forces applied to the load were given, neither was a specific path to follow. These specifications become particularly relevant in cooperative transportation. Consequently, we address here the problem of learning force and position constraints in human-robot cooperative transportation, where the start and target locations of the load vary.

III. PROBLEM FORMULATION

The problem tackled in this paper is that of a human and a robot cooperatively transporting an object from a start location to a target position. Moreover, we consider the case in which the given object should be manipulated with some desired forces, i.e., the forces applied to the load should allow the object to be transported by pressing it on the sides without breaking it. In this context, the robot needs not only to follow a specific trajectory in its workspace, but also to physically interact with the user through the transported load, under some force and position constraints. To formalize the problem, let us consider the operational space dynamics model of the robot under interaction with the environment as

$$\boldsymbol{\Lambda}(\boldsymbol{x})\ddot{\boldsymbol{x}} + \boldsymbol{\mu}(\boldsymbol{x},\dot{\boldsymbol{x}}) + \boldsymbol{p}(\boldsymbol{x}) = \boldsymbol{F} - \boldsymbol{F}_e, \qquad (1)$$

where $\boldsymbol{\Lambda}(\boldsymbol{x})$, $\boldsymbol{\mu}(\boldsymbol{x},\dot{\boldsymbol{x}})$ and $\boldsymbol{p}(\boldsymbol{x})$ are the inertia matrix, the vector of centrifugal and Coriolis forces, and the gravity components, respectively. The pose of the robot is denoted by $\boldsymbol{x}$ (i.e., position and orientation of the end-effector), $\boldsymbol{F}$ is the generalized forces vector, and $\boldsymbol{F}_e$ is the vector of contact forces exerted by the end-effector on the environment. We assume a perfect nonlinear dynamic coupling, which means the robot's end-effector can be treated as equivalent to a single unit mass moving in the Cartesian space [23].

This allows us to formulate our problem as the case of finding the generalized force vector $\boldsymbol{F}$ to attain the desired task dynamics. To achieve this aim, we propose that the robot behavior during the interaction is driven by a virtual attractor represented as a spring-damper system, as shown in Fig. 2. Specifically, the desired robot's motion during interaction is given by

$$\ddot{\boldsymbol{x}} \;=\; \boldsymbol{K}^{\mathcal{P}}(\boldsymbol{y}-\boldsymbol{x}) - \boldsymbol{K}^{\mathcal{V}}\dot{\boldsymbol{x}} - \boldsymbol{F}_e, \qquad (2)$$

where $\boldsymbol{K}^{\mathcal{P}}$, $\boldsymbol{K}^{\mathcal{V}}$ and $\boldsymbol{y}$ are the stiffness matrix, the damping and the path of the virtual attractor, respectively. The learning problem is, therefore, formulated as estimating the path of $\boldsymbol{y}$ that will induce the end-effector to follow the cooperative behaviors demonstrated by the teacher.

Notice that $\boldsymbol{x}$, and its first and second time derivatives are directly obtained from demonstrations. Also, the contact forces $\boldsymbol{F}_e$ are provided by a force sensor mounted at the robot's end-effector. It is worth highlighting that the sensor readings depend on the forces applied by the human and the robot while moving the load, in other words, the sensed forces contain information about the desired force to be applied to the object.

IV. LEARNING AND REPRODUCTION

We propose to probabilistically encode the set of demonstrations through a task-parametrized version of the Gaussian mixture model [7]. Such a model allows us to consider the task constraints given at different frames of reference (i.e., the parameters of the task). Formally, the task parameters are represented as P coordinate systems, defined at time step n by $\{\boldsymbol{b}_{n,j}, \boldsymbol{A}_{n,j}\}_{j=1}^{P}$, representing respectively the origin of the frame and a set of basis vectors $\{\boldsymbol{e}_1, \boldsymbol{e}_2, \ldots\}$ forming a transformation matrix $\boldsymbol{A} = [\boldsymbol{e}_1 \boldsymbol{e}_2 \cdots]$.

A movement is observed from these different viewpoints, forming a third order tensor dataset $\boldsymbol{\mathcal{X}} \in \mathbb{R}^{D\times N\times P}$, composed of P trajectory samples $\boldsymbol{X}^{(j)} \in \mathbb{R}^{D\times N}$. Every $\boldsymbol{X}^{(j)}$ corresponds to a matrix composed of D-dimensional observations at N time steps. In our application[1], $D = 4$,

[1]For sake of simplicity, the end-effector orientation was not considered in the experiments.

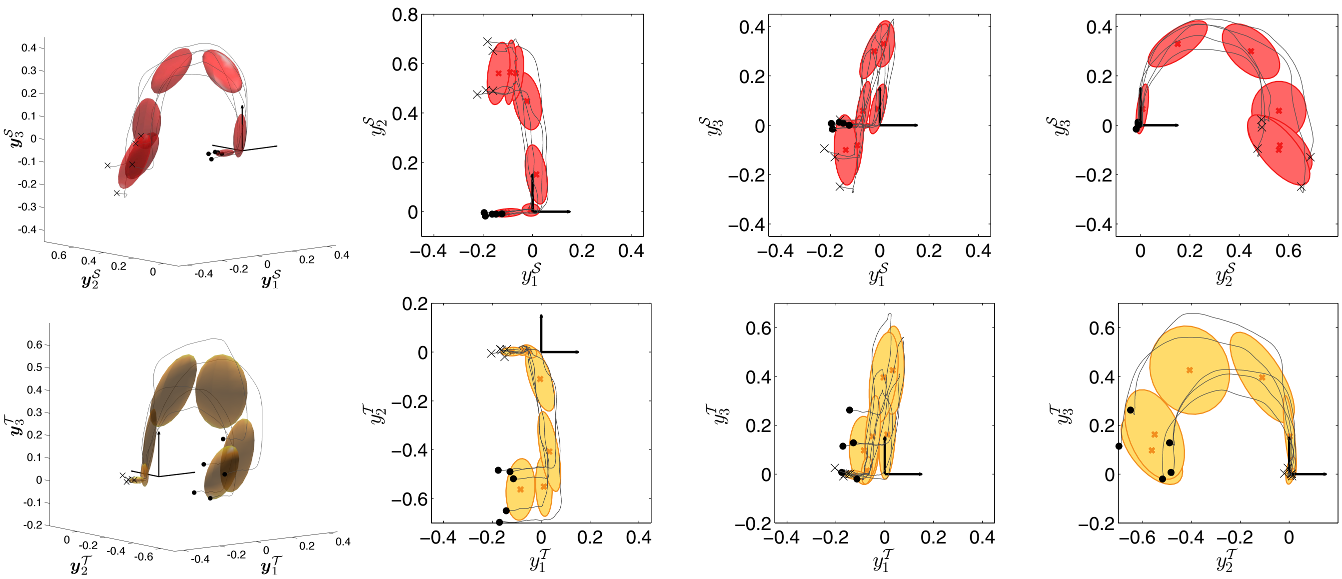

Fig. 4: Probabilistic encoding of the demonstrations at the different candidates frames of the task. The first row shows the model in the *start* frame $\mathcal{S}$, while the second row displays the GMM in the *target* frame $\mathcal{T}$. The gray lines depict the attractor trajectories observed from the corresponding candidate frame. The ellipsoids represent the components of the model.

corresponding to the aggregation of the time variable t and the Cartesian position of the attractor $\boldsymbol{y}$, therefore $\boldsymbol{X}^{(j)} = \begin{bmatrix} t_1 & \dots & t_N \\ \boldsymbol{y}_1^{(j)} & \dots & \boldsymbol{y}_N^{(j)} \end{bmatrix}$. The parameters of the model with K components are defined by $\{\pi_i, \{\boldsymbol{\mu}_i^{(j)}, \boldsymbol{\Sigma}_i^{(j)}\}_{j=1}^{P}\}_{i=1}^{K}$, where π_i are the mixing coefficients, $\boldsymbol{\mu}_i^{(j)}$ and $\boldsymbol{\Sigma}_i^{(j)}$ are the mode-j center and covariance matrix of the i-th Gaussian component.

Learning of the parameters is achieved by setting the constrained problem of maximizing the log-likelihood under the constraints that the data in the different frames are generated from the same source, resulting in an EM process to iteratively update the model parameters until convergence.

E-step:

$$\gamma_{n,i} = \frac{\pi_i \prod_{j=1}^{P} \mathcal{N}\big(\boldsymbol{X}_n^{(j)} |\, \boldsymbol{\mu}_i^{(j)}, \boldsymbol{\Sigma}_i^{(j)}\big)}{\sum_{k=1}^{K} \pi_k \prod_{j=1}^{P} \mathcal{N}\big(\boldsymbol{X}_n^{(j)} |\, \boldsymbol{\mu}_k^{(j)}, \boldsymbol{\Sigma}_k^{(j)}\big)}.$$

M-step:

$$\pi_i = \frac{\sum_{n=1}^{N} \gamma_{n,i}}{N}, \quad \boldsymbol{\mu}_i^{(j)} = \frac{\sum_{n=1}^{N} \gamma_{n,i}\, \boldsymbol{X}_n^{(j)}}{\sum_{n=1}^{N} \gamma_{n,i}},$$

$$\boldsymbol{\Sigma}_i^{(j)} = \frac{\sum_{n=1}^{N} \gamma_{n,i}\, (\boldsymbol{X}_n^{(j)} - \boldsymbol{\mu}_i^{(j)})(\boldsymbol{X}_n^{(j)} - \boldsymbol{\mu}_i^{(j)})^{\top}}{\sum_{n=1}^{N} \gamma_{n,i}}. \quad (3)$$

The learned model can be used to reproduce movements in new situations (for new positions and orientations of candidate frames). The model first retrieves at each time step n a GMM, by computing a product of linearly transformed Gaussians

$$\mathcal{N}(\boldsymbol{\mu}_{n,i}, \boldsymbol{\Sigma}_{n,i}) \propto \prod_{j=1}^{P} \mathcal{N}\Big(\boldsymbol{A}_{n,j}\boldsymbol{\mu}_i^{(j)} + \boldsymbol{b}_{n,j},\ \boldsymbol{A}_{n,j}\boldsymbol{\Sigma}_i^{(j)}\boldsymbol{A}_{n,j}^{\top}\Big),$$

$$\Leftrightarrow \boldsymbol{\Sigma}_{n,i} = \Big(\sum_{j=1}^{P} \big(\boldsymbol{A}_{n,j}\boldsymbol{\Sigma}_i^{(j)}\boldsymbol{A}_{n,j}^{\top}\big)^{-1}\Big)^{-1}, \quad (4)$$

$$\boldsymbol{\mu}_{n,i} = \boldsymbol{\Sigma}_{n,i} \sum_{j=1}^{P} (\boldsymbol{A}_{n,j}\boldsymbol{\Sigma}_i^{(j)}\boldsymbol{A}_{n,j}^{\top})^{-1} (\boldsymbol{A}_{n,j}\boldsymbol{\mu}_i^{(j)} + \boldsymbol{b}_{n,j}).$$

The model parameters are initialized with a *k-means* procedure redefined using a similar process to that used for the modified EM algorithm.

By using the temporary GMM parameters computed in Eq. (4) for a given set of task parameters, we resort to Gaussian mixture regression to retrieve, at each time step, the attractor position during reproduction. Specifically, GMR relies on the joint distribution $\mathcal{P}(t, \boldsymbol{y})$ learned by the task-parametrized GMM. The conditional probability $\mathcal{P}(\boldsymbol{y}_n | t_n)$ is estimated as an output distribution $\mathcal{N}(\hat{\boldsymbol{\mu}}_n^{\boldsymbol{y}}, \hat{\boldsymbol{\Sigma}}_n^{\boldsymbol{y}})$ that is also Gaussian, with

$$\hat{\boldsymbol{\mu}}_n^{\boldsymbol{y}} = \sum_i h_{n,i}(t_n) \left[\boldsymbol{\mu}_{n,i}^{\boldsymbol{y}} + \boldsymbol{\Sigma}_{n,i}^{\boldsymbol{y}t} (\boldsymbol{\Sigma}_{n,i}^{t})^{-1} (t_n - \boldsymbol{\mu}_{n,i}^{t}) \right],$$

$$\hat{\boldsymbol{\Sigma}}_n^{\boldsymbol{y}} = \sum_i h_{n,i}^2(t_n) \left[\boldsymbol{\Sigma}_{n,i}^{\boldsymbol{y}} - \boldsymbol{\Sigma}_{n,i}^{\boldsymbol{y}t} (\boldsymbol{\Sigma}_{n,i}^{t})^{-1} \boldsymbol{\Sigma}_{n,i}^{t\boldsymbol{y}} \right], \quad (5)$$

and activation weights $h_{n,i}(t_n)$ defined as

$$h_{n,i}(t_n) = \frac{\pi_i \mathcal{N}(t_n |\, \boldsymbol{\mu}_i^{t}, \boldsymbol{\Sigma}_i^{t})}{\sum_k^K \pi_k \mathcal{N}(t_n |\, \boldsymbol{\mu}_k^{t}, \boldsymbol{\Sigma}_k^{t})}.$$

V. TRANSPORTATION EXPERIMENT

We test the performance of our approach in an experiment where a human-robot dyad transports an object from a start location to a desired target. The detailed description about the setting, the demonstration and reproduction phases as well as the obtained results are given below.

A. Description of the task

At the beginning of the transportation task, two participants simultaneously reach for the object. Once they make contact with the load, they start jointly transporting the object along a given path to reach the target location. When the object gets to the final position, the human-human pair releases it and moves away from the object. Note that both the starting and goal object position/orientation may vary across repetitions. As stated in Section I, the aim is to introduce a robot into such a task by replacing one of the human participants by a robot.

Specifically, we used a torque-controlled 7 DOFs WAM robot fitted with a 6-axis force/torque sensor. In the demonstration phase, the gravity-compensated robot is kinesthetically guided by the teacher while cooperatively achieving the task with the other human partner, as shown in Figure 1. Five examples of collaborative behavior are given to the robot. The teacher shows the robot both the path to be followed and the force pattern it should use while transporting the load (see Figure 3). The demonstrations are then used for training a five-states task-parametrized GMM ($K = 5$, selected empirically) with two candidate coordinate systems ($P = 2$), namely, the frames representing the start and target locations of the object. They are respectively defined as[2]

$$\boldsymbol{A}_{n,1} = \begin{bmatrix} 1 & \mathbf{0}^{\top} \\ \mathbf{0} & \boldsymbol{R}^{\mathcal{S}} \end{bmatrix}, \boldsymbol{b}_{n,1} = \begin{bmatrix} 0 \\ \boldsymbol{x}_o^{\mathcal{S}} \end{bmatrix},$$

and

$$\boldsymbol{A}_{n,2} = \begin{bmatrix} 1 & \mathbf{0}^{\top} \\ \mathbf{0} & \boldsymbol{R}^{\mathcal{T}} \end{bmatrix}, \boldsymbol{b}_{n,2} = \begin{bmatrix} 0 \\ \boldsymbol{x}_o^{\mathcal{T}} \end{bmatrix}.$$

Here, $\boldsymbol{R}^{\mathcal{S}}$ and $\boldsymbol{R}^{\mathcal{T}}$ respectively represent the start and final orientation of the object with rotation matrices, while $\boldsymbol{x}_o^{\mathcal{S}}$ and $\boldsymbol{x}_o^{\mathcal{T}}$ define its corresponding Cartesian positions.[3] Finally, the attractor's trajectory is computed using Eq. (2) with predefined values for the matrices $\boldsymbol{K}^{\mathcal{P}} = 500 \cdot \boldsymbol{I}$ and $\boldsymbol{K}^{\mathcal{V}} = 60 \cdot \boldsymbol{I}$.

During reproduction of the task, the start and target frames are given to the model in order to obtain the temporary GMM parameters using Eq. (4). Then, the robot and its human partner transport the object towards the target location. Here, for each time step t_n, the robot obtains a new attractor location from Eq. (5) (as explained in Section III), that generates a new desired acceleration in the operational space of the robot. For sake of simplicity in the experiments, the orientation of the robot's end-effector is fixed.

B. Results

Fig. 4 shows the resulting encoding of the attractor trajectories computed from Eq. (2) and observed from the two different candidate frames. Notice how the multiple demonstrations are locally consistent when the robot approaches

[2]Note that the duration of the task is not modulated by the task parameters.

[3]The position and orientations of the object were predefined in the experiment, but these can alternatively be obtained using a vision or optical tracking system. Information regarding the motion of the human partner was not considered here.

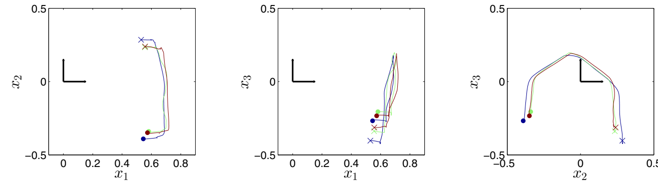

(a) Reproductions with varying start and target locations of the object.

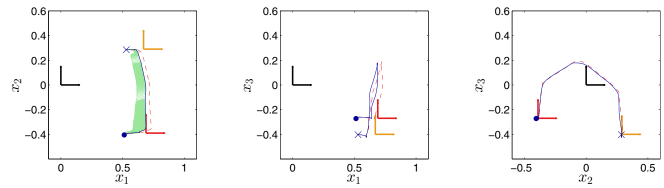

(b) Nearly constant force applied by the human partner to the object along the whole reproduction.

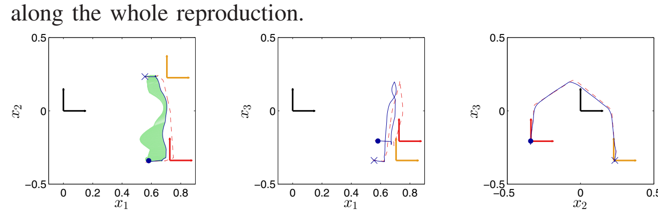

(c) Human varies the applied force along the whole reproduction. The robot adapts accordingly.

Fig. 5: The solid lines represent the robot's trajectory while the dashed lines depict the trajectory of the attractor $\boldsymbol{y}$ obtained from GMR. The green area display the sensed force at the robot's end-effector. The dots and crosses respectively display the start and end of the reproduction.

the start location of the object (i.e., frame $\mathcal{S}$), and when the manipulator moves away once the load has been placed at its target position (i.e., frame $\mathcal{T}$). This is reflected by the small ellipsoids in these parts of the task.

After learning, the obtained model was used to test the reproduction of the task on the real platform. Three different types of tests were carried out to evaluate the performance of the robot. First, the human and robot cooperatively transported the load as demonstrated, i.e., the force applied to the load was similar to those given previously. Fig. 5a shows three successful reproductions under the aforementioned condition where both the starting and target location varied. Fig. 5b shows one of these reproductions where it is clearly observed that the sensed force profile remains nearly constant throughout the whole reproduction. It is worth highlighting that the observed offset between the end-effector position and the attractor path allows the robot to apply the desired force to the load while transporting it.

The second test consisted of applying a varying force to evaluate how the robot reacted to force perturbations not observed during learning. The human operator started the task pushing the object with a force higher than those taught during the demonstrations. Then, the applied force was significantly reduced, and finally it reached values similar to the demonstrations, as shown in Fig. 5c. It is observed that the robot could successfully adapt to these force variations.

When the force is high, the robot behaves compliantly, allowing small deviations from the path, still ensuring that the position constraint remains within a feasible range determined by the observed variability in the demonstrations and the controller gains. In contrast, when the force is very low (i.e., the human may be losing the contact with the load), the robot moves to apply more force and prevent the object from being dropped. Note that despite the force variations, the robot was able to transport the object along a similar path in the other dimensions, by showing a collaborative behavior that is an appropriate compromise between force and position constraints, automatically extracted from the statistical representation of the demonstrations.

The last test concerned the situation in which the human completely releases the object. In this case, the robot's end-effector moved forward, but only within a boundary defined by the variations of the demonstrated possible paths. In other words, the robot does not push indefinitely, but it instead moves in an appropriate manner according to the unexpected circumstances and its prior knowledge of the task learned from the demonstrations. A video of the experiment and the task-parameterized GMM sourcecode are available at `http://programming-by-demonstration.org/Roman2014/`.

VI. CONCLUSIONS AND FUTURE WORK

We presented a PbD approach for teaching a robot to cooperatively transport objects. Our method exploits the advantages of a dynamical system formulation for modelling both the motion and the interaction of the robot with the user and the environment along the task. The dynamics of the system is learned from a set of demonstrations that is encapsulated in a task-parametrized GMM. Note that, in contrast to previous works, the robot extracts the desired path to follow and the needed force to be applied to the load from the examples provided by a human user. Therefore, the approach does not depend on a specific model of the task, but it automatically extracts the different constraints of the problem. The results showed that the robot successfully carried out the task, and that it was able to adapt to force perturbations not observed during the learning phase.

In future work, similarly as in [24], we plan to extend this research towards the estimation of the stiffness and damping matrices of the virtual attractor. In contrast to [6], where only the stiffness gains were estimated through a two-step process, we want to learn the task and estimate stiffness and damping in a one-shot fashion. This would allow the robot to shape its compliance level along the task according to the provided demonstrations. We also plan to explore the variability of the demonstrations encapsulated in the covariance matrices of the model, which could be exploited to detect if the robot reaches an unexpected situation that is too far from the demonstrations (e.g., in case of failures), requiring the user to provide new demonstrations.

REFERENCES

[1] A. Billard, S. Calinon, R. Dillmann, and S. Schaal, "Robot programming by demonstration," in *Springer Handbook of Robotics* (B. Siciliano and O. Khatib, eds.), pp. 1371–1394, Springer, 2008.

[2] B. Akgun, M. Cakmak, J. Yoo, and A. Thomaz, "Trajectories and keyframes for kinesthetic teaching: A human-robot interaction perspective," in *HRI*, pp. 391–398, 2012.

[3] L. Rozo, P. Jiménez, and C. Torras, "A robot learning from demonstration framework to perform force-based manipulation tasks," *Journal of Intelligent Service Robotics, Special Issue on Artificial Intelligence Techniques for Robotics: Sensing, Representation and Action, Part 2*, vol. 6, no. 1, pp. 33–51, 2013.

[4] S. Calinon, P. Evrard, E. Gribovskaya, A. Billard, and A. Kheddar, "Learning collaborative manipulation tasks by demonstration using a haptic interface," in *ICAR*, pp. 1–6, 2009.

[5] J. Medina, M. Lawitzky, A. Mortl, D. Lee, and S. Hirche, "An experience-driven robotic assistant acquiring human knowledge to improve haptic cooperation," in *IROS*, pp. 2416–2422, 2011.

[6] L. Rozo, S. Calinon, D. G. Caldwell, P. Jiménez, and C. Torras, "Learning collaborative impedance-based robot behaviors," in *AAAI Conf. on Artificial Intelligence*, pp. 1422–1428, 2013.

[7] S. Calinon, Z. Li, T. Alizadeh, N. Tsagarakis, and D. Caldwell, "Statistical dynamical systems for skills acquisition in humanoids," in *Humanoids*, pp. 323–329, 2012.

[8] K. Kosuge, H. Yoshida, and T. Fukuda, "Dynamic control for robot-human collaboration," in *RO-MAN*, pp. 398–401, 1993.

[9] K. Kosuge and N. Kazamura, "Control of a robot handling an object in cooperation with a human," in *RO-MAN*, pp. 142–147, 1997.

[10] O. Al-Jarrah and Y. Zheng, "Arm-manipulator coordination for load sharing using reflexive motion control," in *ICRA*, pp. 2326–2331, 1997.

[11] V. Duchaine and C. Gosselin, "General model of human-robot cooperation using a novel velocity based variable impedance control," in *EuroHaptics*, pp. 446–451, 2007.

[12] R. Ikeura and H. Inooka, "Variable impedance control of a robot for cooperation with a human," in *ICRA*, pp. 3097–3102, 1995.

[13] J. Dumora, F. Geffard, C. Bidard, and P. Fraisse, "Towards a robotic partner for collaborative manipulation," in *HRI - Workshop on Collaborative Manipulation*, pp. 1–6, 2013.

[14] J. Dumora, F. Geffard, C. Bidard, T. Brouillet, and P. Fraisse, "Experimental study on haptic communication of a human in a shared human-robot collaborative task," in *IROS*, pp. 5137–5144, 2012.

[15] R. Ikeura, T. Moriguchi, and K. Mizutani, "Optimal variable impedance control for a robot and its application to lifting an object with a human," in *RO-MAN*, pp. 500–505, 2002.

[16] M. Rahman, R. Ikeura, and K. Mizutani, "Investigating the impedance characteristic of human arm for development of robots to cooperate with human operators," in *IEEE Intl. Conf. on Systems, Man and Cybernetics*, pp. 676–681, 1999.

[17] T. Flash and N. Hogan, "The coordination of arm movements: An experimentally confirmed mathematical model," *Journal of Neuroscience*, vol. 5, no. 7, pp. 1688–1703, 1985.

[18] Y. Maeda, T. Hara, and T. Arai, "Human-robot cooperative manipulation with motion estimation," in *IEEE/RSJ Intl. Conf. on Intelligent Robots and Systems (IROS)*, pp. 2240–2245, 2001.

[19] T. Tsumugiwa, R. Yokogawa, and K. Hara, "Variable impedance control based on estimation of human arm stiffness for human-robot cooperative calligraphic task," in *ICRA*, pp. 644–650, 2002.

[20] C. Parker and E. Croft, "Design and personalization of a cooperative carrying robot controller," in *ICRA*, pp. 3916–3921, 2012.

[21] D. Kulić, W. Takano, and Y. Nakamura, "Incremental learning, clustering and hierarchy formation of whole body motion patterns using adaptive hidden Markov chains," *IJRR*, vol. 27, no. 7, pp. 761–784, 2008.

[22] E. Gribovskaya, A. Kheddar, and A. Billard, "Motion learning and adaptive impedance for robot control during physical interaction with humans," in *ICRA*, pp. 4326–4332, 2011.

[23] O. Khatib, "A unified approach for motion and force control of robot manipulators: The operational space formulation," *IEEE Journal on Robotics and Automation*, vol. 3, no. 1, pp. 43–53, 1987.

[24] S. Calinon, D. Bruno, and D. G. Caldwell, "A task-parameterized probabilistic model with minimal intervention control," in *ICRA*, (Hong Kong, China), May-June 2014.